Photocyclization of *N*,*N*′-diphenyl-1-hydroxy-9,10-anthraquinone diimines *via* excited-state intramolecular proton transfer (ESIPT)

Keiji Kobayashi,*,[a] Mayumi Iguchi,[a] Tatsuro Imakubo,[a] Koichi Iwata[b] and Hiro-o Hamaguchi[b]

[a] *Department of Chemistry, Graduate School of Arts and Sciences, The University of Tokyo, Komaba, Meguro-ku, Tokyo 153-8902, Japan*
[b] *Department of Chemistry, Graduate School of Science, The University of Tokyo, Hongo, Bunkyo-ku, Tokyo 113-8654, Japan*

Photolysis of 1,5-dihydroxy- and 1-hydroxy-substituted *N*,*N*′-diphenyl-9,10-anthraquinone diimines (1a and 1b) produces acridine-condensed ring systems due to oxidative cyclization. In contrast, anthraquinone diimines which bear no hydroxy group on the C1-position show no photoreactivity, providing chemical evidence for participation of excited-state intramolecular proton transfer (ESIPT) in the photocyclization. The ground-state of 1a includes only a small fraction (*ca.* 4%) of the keto enamine form in fast equilibrium with the enol imine form, as proved by temperature dependent ^{1}H and ^{13}C NMR spectroscopy. An X-ray crystal analysis of 1a reveals that the molecule exists in the crystalline state as the enol imine form with a butterfly conformation of the anthraquinone ring. The involvement of ESIPT in photoexcited 1a has been revealed by means of sub-microsecond time-resolved IR spectroscopy. Upon irradiation of 1a an increase of the ground-state keto form (B) is detected and its lifetime is deduced to be 1.3 ms. Another transient species (A) with a lifetime of 80 μs is also observed, which is assumed to be the intramolecular cycloadduct as a precursor of the photoproduct.

Excited state intramolecular proton transfer (ESIPT) has elicited considerable experimental and theoretical interest.[1] The majority of recent research on ESIPT systems has been devoted to photophysics in relation to photochromic materials and UV-stabilizers of salicylates[2] and salicylideneanilines.[3] The photoexcited state *via* ESIPT is deactivated, in general, non-radiatively and/or radiatively to the ground state of the tautomeric keto form which regenerates thermally the original phenolic form. In such a photophysical cycle, the ESIPT-induced excited state will produce the ground-state keto form and other chemical deactivation processes have rarely been encountered except for *cis–trans* isomerizations of the C=N bond of salicylideneanilines. Photoreactions which proceed *via* ESIPT have been reported so far for *o*-allylphenol,[4] *o*-ethynylphenol[5] and benzylidene(*o*-hydroxy)aniline.[6] Recently we have reported the first example, to the best of our knowledge, of a photochemical reaction *via* ESIPT in photo-tautomeric systems such as salicylates or salicylideneanilines.[7] We describe herein the full details of the ESIPT system that includes an irreversible photochemical reaction as a deactivation path.

In this work we introduce submicrosecond time-resolved vibrational spectroscopy to detect transient species. Transient absorption and emission spectroscopies have been extensively employed in the study of the ESIPT systems,[8] while investigation by the use of vibrational spectroscopy is still in its infancy.[9] This tool has been proved to be quite useful in shedding light on fast reactions, particularly on those including a change in the functional groups as described in this investigation.

Experimental

General methods

^{1}H and ^{13}C NMR spectra were recorded at 500 MHz in $CDCl_3$ unless specified otherwise and are reported in ppm units with TMS as internal standard. *J* values are given in Hz. IR spectra were obtained on a Jasco FT/IR-350 infrared spectrometer. UV–VIS spectra were obtained on a Hitachi U-3200 spectrometer. Mass spectra were taken by a direct insertion probe at ionizing voltage of 70 eV with electron-impact ionization. Benzene used for preparative-scale photolysis was purified by refluxing with calcium hydride and distillation under nitrogen. Carbon tetrachloride was dried by calcium hydride and distilled prior to use for time-resolved experiments.

N,*N*′-Diphenyl-1,5-dihydroxy-9,10-anthraquinone diimine (1a)

To a solution of 1,5-dihydroxy-9,10-anthraquinone (201 mg, 0.873 mmol) and aniline (1.5 cm^3, 16.5 mmol) in benzene (20 cm^3) was added 0.36 cm^3 (3.3 mmol) of $TiCl_4$ dropwise *via* a pipette under an Ar atmosphere. After stirring at room temperature for 3 h, the solution was refluxed overnight. The cooled mixture was poured into ice–water (50 cm^3) and the resulting solids were removed by filtration. The solid was washed with hot toluene (150 cm^3) and the water layer was extracted twice with toluene (25 cm^3). The organic layer and combined organic extracts were washed twice with saturated Na_2CO_3 solution, once with water and brine, and dried over $MgSO_4$. The solvent was removed *in vacuo* and the crude products were recrystallized from hexane–dichloromethane to give diimine **1a** as deep red prisms (146 mg; 45%), mp 217–218 °C; $\delta_H(CDCl_3)$ 14.41 (s, 2H), 7.38 (t, *J* 7.4, 4H), 7.20 (t, *J* 7.4, 2H), 7.07–7.02 (m, 8H), 6.80 (dd, *J* 6.8, 2.0, 2H); $\delta_C(CDCl_3)$ 160.7, 160.4, 147.9, 131.1, 129.8, 128.5, 125.1, 120.8, 120.7, 120.6, 118.6; ν_{max}(KBr)/cm^{-1} 3453 (O–H), 1580.4 (C=N); $\lambda_{max}(CH_2Cl_2)$/nm (ε/dm^3 mol^{-1} cm^{-1}) 233 (99 000), 296 (35 000), 394 (23 000); *m*/*z* 390 (M^+), 373 ($M^+ - OH$); elemental microanalysis (%): Found (Calc.): C, 79.86 (79.98); H, 4.97 (4.65); N, 7.28 (7.17).

N,*N*′-Diphenyl-1-hydroxy-9,10-anthraquinone diimine (1b)

This compound was prepared according to the method described for **1a**, by using 1-hydroxy-9,10-anthraquinone (1.90 g, 8.48 mmol), $TiCl_4$ (3.0 cm^3, 27 mmol) and aniline (12.0 cm^3, 132 mmol), as yellowish brown needles (2.72 g; 81%), mp

187–189 °C (decomp.); $\delta_H(CDCl_3)$ 14.26 (br s), 13.96 (br s), 7.38–6.66 (br m); $\delta_C(CDCl_3)$ 160.6–116.8 (br 36 signals); ν_{max}(KBr)/cm^{-1} 3431 (O–H), 1630 (C=N), 1586 (H-bonded C=N); $\lambda_{max}(CH_2Cl_2)$/nm (ε/dm^3 mol^{-1} cm^{-1}) 234 (42 000), 289 (21 000), 394 (8600); *m*/*z* 374 (M^+), 357 ($M^+ - OH$); elemental microanalysis (%): Found (Calc.): C, 83.47 (83.40); H, 5.09 (4.85); N, 7.61 (7.48).

Anthraquinone diimine (1c) and 1,5-dimethoxyanthraquinone diimine (1d)

These were prepared according to the procedure reported previously.[10]

Photolysis

Benzene in a quartz container was deaerated by bubbling with argon gas for 30 min. To this 80 mg (0.205 mmol) of **1a** was added and mixed to prepare a solution of *ca.* 8×10^{-4} molar concentration. The solution was irradiated with a 100 W high pressure mercury lamp through a Pyrex filter. After irradiation for 48 h the solvent was removed under vacuum and the residual oil was chromatographed on a silica gel column with hexane–dichloromethane (1 : 1) as eluent to give **2a** (51 mg; 64%) and **3** (3.5 mg; 4%). **2a**: Red prisms, mp >300 °C; $\delta_H(CD_2Cl_2)$ 17.10 (s, 1H), 16.47 (s, 1H), 8.71 (d, *J* 9.6, 1H), 8.54 (d, *J* 6.7, 1H), 8.16 (d, *J* 7.8, 1H), 7.74 (t, *J* 7.6, 1H), 7.71 (t, *J* 6.9, 1H), 7.47 (d, *J* 9.6, 1H), 7.38 (t, *J* 6.8, 2H), 7.31 (d, *J* 8.2, 1H), 7.27–7.16 (m, 5H); $\delta_C(CDCl_3)$ 176.8, 161.9, 158.9, 147.8, 142.8, 140.1, 130.7, 130.3, 130.2, 129.9, 128.3, 128.1, 127.7, 126.9, 126.5, 124.2, 124.1, 123.5, 121.6, 121.3, 120.6, 120.5, 117.8, 109.1; ν_{max}(KBr)/cm^{-1} 3448 (br, O–H and N–H), 1618 (C=O), 1551 (C=N); $\lambda_{max}(CH_2Cl_2)$/nm (ε/dm^3 mol^{-1} cm^{-1}) 236 (33 000), 273 (27 000), 359 (6200), 421 (5700), 499 (8400), 528 (9800); *m*/*z* 388 (M^+), 371 ($M^+ - OH$). **3**: Dark brown powder, $\delta_H(CDCl_3)$ 17.46 (s, 2H), 8.73 (d, *J* 9.2, 2H), 8.54 (d, *J* 8.7, 2H), 8.13 (d, *J* 7.8, 2H), 7.78 (d, *J* 9.2, 2H), 7.74 (t, *J* 7.3, 2H), 7.70 (t, *J* 5.0, 2H); ν_{max}(KBr)/cm^{-1} 3432 (br O–H and N–H), 1617 (br C=O); $\lambda_{max}(CH_2Cl_2)$/nm (ε/dm^3 mol^{-1} cm^{-1}) 242 (40 000), 266 (21 000), 311 (12 000), 336 (3700), 355 (4600), 372 (5400), 391 (2700), 440 (3900), 467 (8700), 497 (12 000), 527 (3000), 569 (3800); *m*/*z* 386 (M^+).

Photolysis of a 1.04 mmol solution of **1b** in benzene for 54 h afforded **2b** (17 mg; 18%) as red powder. **2b**: $\delta_H(CD_2Cl_2)$ 17.08 (s, 1H), 9.47 (br, d, 1H), 8.70 (d, *J* 9.5, 1H), 8.52 (d, *J* 8.2, 1H), 8.39 (br, 1H), 7.80–7.53 (m, 4H), 7.47 (d, *J* 9.5, 1H), 7.45 (d, *J* 9.8, 2H), 7.34–7.28 (m, 4H); $\delta_C(CDCl_3)$ 176.9, 158.3, 144.4, 143.9, 142.8, 136.7, 136.6, 131.8, 130.6, 129.8, 129.6, 128.8, 128.2, 127.7, 127.5, 126.7, 126.3, 126.1, 124.5, 124.3, 123.5, 121.4, 120.4, 108.9; ν_{max}(KBr)/cm^{-1} 3434 (br N–H), 1617 (C=O), 1564 (br C=N); *m*/*z* 372 (M^+), 355.

X-Ray crystallographic analyses of 1a and 2a

Intensity data were collected at 295 K on a Rigaku AFC-7R diffractometer (Cu-Kα radiation, $\lambda = 1.541\,84$ Å) for **1a** and a Rigaku AFC-5S diffractometer (Mo-Kα, $\lambda = 0.710\,73$ Å) for **2a**. The crystal structures were solved by direct methods using the SIR 88 program[11b] and the refinement was carried out using the teXsan computer program.[11a] The H(–N) and H(–O) atoms were located from difference Fourier maps but other H-atoms were fixed geometrically. All non-H atoms were refined anisotropically and the H-atoms were not included in refinement. Crystal data for **1a**: $C_{26}H_{18}N_2O_2$, $M_w = 390.44$, monoclinic, $P2_1/n$, $a = 10.550(3)$, $b = 18.923(3)$, $c = 11.184(2)$ Å, $\beta = 115.10(1)°$, $U = 2021.9(7)$ Å^3, $Z = 4$, $D_c = 1.283$ g cm^{-3}, 3305 reflections measured in the range $4 < 2\theta < 55$, 2610 unique reflections with $|I| > 3\sigma|I|$. $R = 0.055$ and $R_w = 0.069$. Crystal data for **2a**: $C_{26}H_{16}N_2O_2$, $M_w = 388.42$, triclinic, space group $P\bar{1}$, $a = 11.020(1)$, $b = 11.377(1)$, $c = 8.746(1)$ Å, $\alpha = 110.65(1)$, $\beta = 94.00(1)$, $\gamma = 113.73(1)°$, $U = 910.0(2)$ Å^3, $Z = 2$, $D_c = 1.417$ g cm^{-3}, 4399 reflections measured in the range $4 < 2\theta < 55$, 1436 unique reflections with $|I| > 3\sigma|I|$. $R = 0.045$ and $R_w = 0.026$. Full crystallographic details, excluding structure factor tables, have been deposited at the Cambridge Crystallographic Data Centre (CCDC). For details of the deposition scheme, see 'Instructions for Authors', *J. Chem. Soc.*, *Perkin Trans. 2*, available *via* the RSC Web page (http://www.rsc.org/authors). Any request to the CCDC for this material should quote the full literature citation and the reference number 188/139 for **1a** and 182/764 for **2a**.

Time-resolved IR spectroscopy

The sub-microsecond time-resolved infrared system consists of a dispersive IR spectrometer, a photoconductive-type MCT detector, an ultra-low noise ac preamplifier with ultra-stable power supplies, a second stage amplifier, a box car integrator, a digital oscilloscope and a personal computer. The photo-excitation of the sample is performed by the fourth harmonic (wavelength 262 nm, pulse width 5 ns, average power 50 mW, repetition rate 1 kHz) of a diode-laser pumped Nd:YLF laser. Details have been described previously.[12]

Results and discussion

Ground-state structure

The ESIPT system employed in this work is *N*,*N*′-diphenyl-1,5-dihydroxy-9,10-anthraquinone diimine **1a**, which is composed of two benzilidenaniline moieties. In order to obtain insights into the ESIPT behaviour of **1a**, it is necessary to see if the enol imine–keto enamine tautomerism is involved in the ground

enol imine keto enamine

state. At the outset of this study we determined the molecular structure of **1a** in the solid-state by an X-ray crystal analysis. The molecular structure is illustrated in Fig. 1. The two *N*-phenyl groups are arranged in an *anti* configuration with each other and are directed to the *peri*-hydrogen atoms rather than to the *peri*-hydroxy substituents. This orientation of the phenyl substituents allows the OH···N intramolecular hydrogen bond to form, as recognized in the IR absorption band of 3450 cm^{-1}. The molecular conformation of **1a** is in sharp contrast with that of the 1,4-dimethoxy derivative **1d**, in which the two *N*-phenyl rings lie above the methoxy substituents.[10] The central anthraquinone framework adopts a butterfly shape, being buckled by 26°, as shown in the end-on-view of the molecular structure of Fig. 1(b). This buckling angle is the same as that of the unsubstituted diimine **1c**,[13] and is 8° larger than that of the 1,4-methoxy derivative **1d**.[10] The *peri*-OH groups in **1a** would have a role in retaining molecular planarity due to the intramolecular hydrogen bonds rather than exerting steric hindrance, leading to molecular buckling.

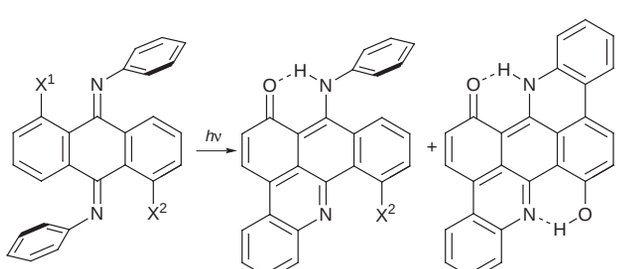

1a : $X^1 = X^2 = OH$ **2a** : $X^2 = OH$ **3**
1b : $X^1 = OH$, $X^2 = H$ **2b** : $X^2 = H$
1c : $X^1 = X^2 = H$
1d : $X^1 = X^2 = OMe$

The carbon–oxygen bond lengths, 1.395(5) and 1.365(4) Å, are consistent with a C–O single bond rather than a carbonyl C=O double bond. On the other hand, the N–C (central ring)

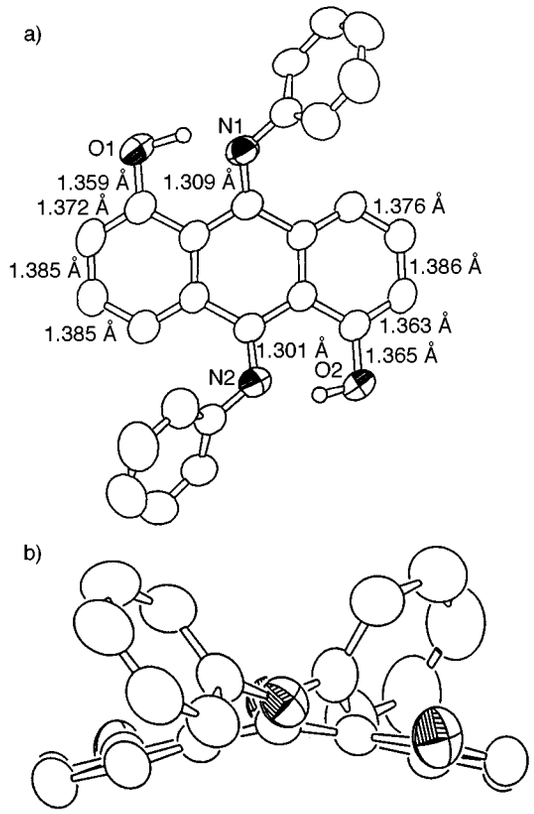

Fig. 1 (a) Molecular structure of **1a** along with selected bond lengths. (b) The end-on-view of **1a** to illustrate the buckling of the anthraquinone ring system.

bonds, 1.309(5) and 1.301(5) Å, are represented by the imino C=N linkage rather than the amino C–N bond.[14] The bond alternation is small in the hydroxy-substituted benzene rings. All of the above observations indicate that **1a** exists essentially as an enol imine form in the solid-state.

To examine the possibility of ground-state tautomerization in solution, variable-temperature NMR studies were carried out for compound **1a** over a temperature range of −90 to 100 °C. The change in the ^{1}H NMR spectra is shown in Fig. 2. With a decrease in temperature, only the signals due to 2-H and 6-H undergo a high-field shift (from δ 6.80 to 6.66, $\Delta = -0.14$ ppm), while the other peaks exhibit no change. Throughout the temperature change no additional peaks appear. Thus there is a fast equilibrium between the enol imine and keto enamine forms and the keto enamine form decreases at low temperatures, since the tautomerization to the keto form should cause a significant down-field shift of the α-protons adjacent to the carbonyl groups, *i.e.* 2-H and 6-H. Furthermore, it is evident that the fast tautomerization occurs simultaneously at the two hydroxy groups, since the signals of the 2-H and 6-H protons occur as a single peak.

The ^{13}C NMR spectrum of **1a** measured in $CDCl_3$ consists of two signals at 161.0 and 160.6 ppm, the former being ascribed to the averaged signal of the C(=N) and C(–N) carbons and the latter to that of the C(=O) and C(–O) carbons.[15] The signal of the CO carbon moves to higher field with decreasing the temperature (Fig. 3). This is consistent with the variable temperature ^{1}H NMR, indicating that the C–OH character in the enol imine form is increased with lowering temperature.

The enol imine to keto enamine ratio at room temperature was estimated roughly as follows. The intrinsic chemical shift of the keto form was assumed to be the same as that observed in photoproduct **2a** (176.9 ppm) and that of the imine form was 160.0 ppm, that is, the chemical shift observed at the lowest extreme of the temperature (−90 °C) in these measurements. Then, we can estimate the population of n_k and n_i from

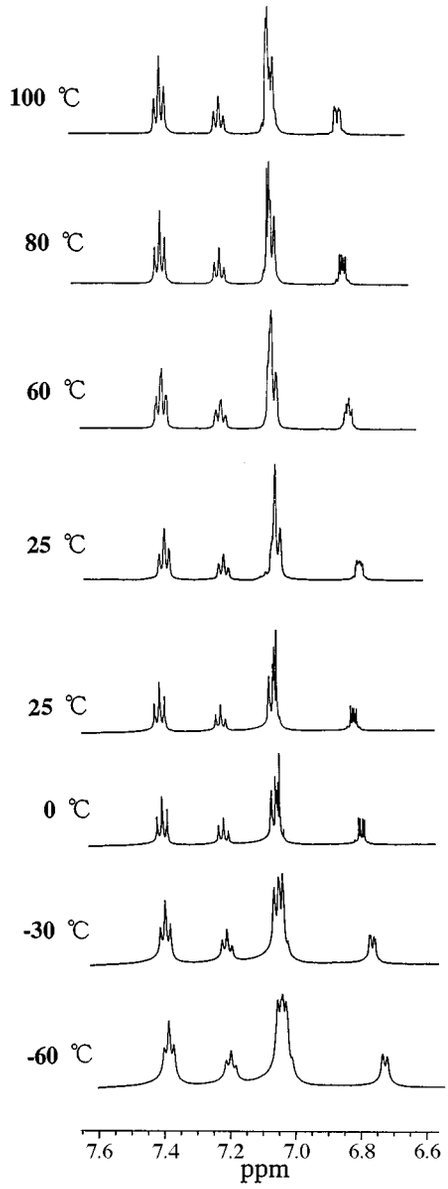

Fig. 2 Variable temperature ^{1}H NMR spectra of **1a** in $CDCl_2$–$CDCl_2$ above room temperature (25–100 °C) and in CD_2Cl_2 below room temperature (−60–25 °C)

eqns. (1) and (2). According to this procedure, we deduced

$$v_o(160.6) = n_k v_k + n_i v_i \quad (1)$$

$$n_k + n_i = 1 \quad (2)$$

roughly the population of the keto enamine form at room temperature to be about 4%. The IR spectrum of **1a** is consistent with the results of the NMR; the absorption band ascribed to a carbonyl group was not observed.

Photolysis

Compound **1a** exhibits an absorption maximum at 400 nm and its band extends beyond 500 nm. Compound **1a** was irradiated in benzene at room temperature for 48 h. Irradiation experiments were carried out using a 100 W high pressure Hg lamp through a Pyrex filter under argon bubbling. The photoproducts were chromatographed on silica gel to afford acridine-condensed derivatives **2a** and **3** in 64 and 4% yields, respectively. Irradiation of **2a** under the same conditions gave rise to **3**, indicating that **3** is a secondary photoproduct of **1a**. The structure of acridine **2a** was deduced from the spectral data as well

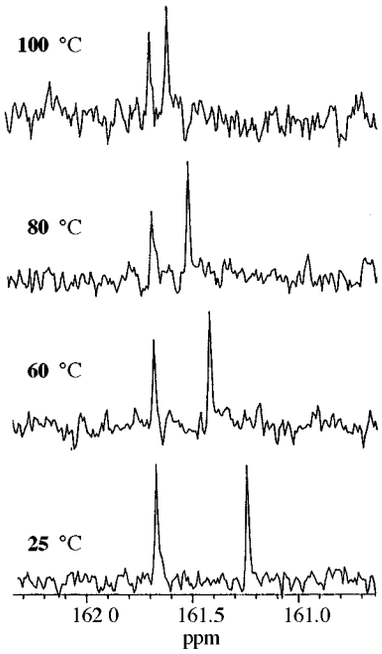

Fig. 3 Variable temperature ^{13}C NMR spectra of **1a** in $CDCl_2$–$CDCl_2$ above room temperature

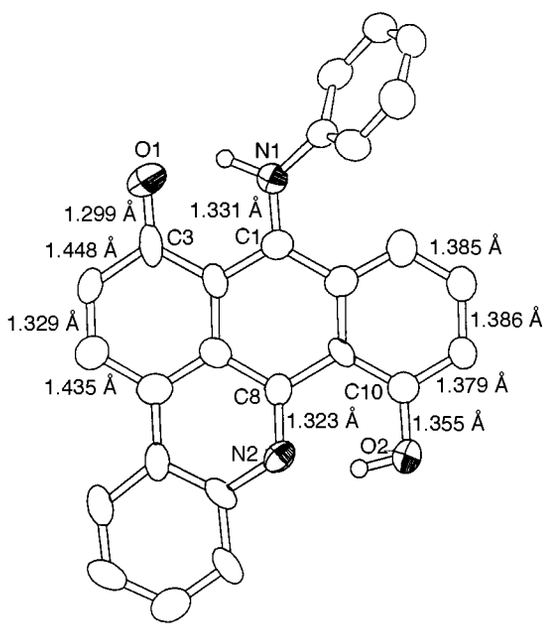

Fig. 4 Molecular structure of **2a** along with selected bond lengths

as from an X-ray crystallographic analysis. A perspective view of the molecular structure of **2a** is shown in Fig. 4. One of the carbon–oxygen bond lengths is 1.299(6) Å, corresponding to the carbonyl C=O bond, while the other is 1.355(6) Å, being ascribed to the C–O single bond. In accordance with the above, the conjugated π-bonds exhibit significant bond alternation on the array close to the carbonyl group, as shown in Fig. 4. The secondary photoproduct was assigned to **3** on the basis of its spectral information; the molecular ion peak of 386 indicates bis-cyclization and the ^1H NMR spectrum suggests a highly symmetrical structure. All of the IR spectral data are consistent with the structure **3**.

The photocyclization was also accomplished in the monohydroxy derivative **1b** to form **2b** in 18%. The structure of **2b** was deduced from the spectral data; monocyclization is evident from the molecular ion peak at 372 in the mass spectrum. Based on HOMO decoupling experiments in ^1H NMR, it was revealed that the two peaks at δ 8.72 and 7.45 are coupled only with each other, indicating that the cyclization of the aniline group occurs to the C-4 position of the anthraquinone framework. The tautomerization of the hydroxy group to form the keto moiety is deduced from the occurrence of the ^{13}C NMR signals due to the carbonyl carbon at δ 176.9 and the IR absorption of the C=O stretching at 1617 cm^{-1}. In contrast to **1a** and **1b**, irradiation of **1c** and **1d**, which bear no hydroxy group at the *peri*-position, caused no photoreactions even after irradiation beyond 60 h.

Both photoproducts **2a** and **2b** are composed of an acridine heterocycle, which is formed by monocyclization at the *para*-position of the hydroxy group. This common characteristic of the photoproducts indicates that the same type of the photoreaction took place in **1a** and **1b**. The absence of photoreactivity in **1c** and **1d** shows clearly that the hydroxy group at the *peri*-position plays an essential role in promoting the photocyclization to the acridine ring compound. Furthermore, the lack of photoreactivity in the methoxy derivative **1d** suggests that the role of the hydroxy substituent is not related to its electron donating nature. These chemical aspects of the photocyclization are best understood by considering the photochemical process *via* excited-state intramolecular proton transfer (ESIPT).

The formation of polycyclic systems by intramolecular photocyclization is a common process for several types of aromatic compounds like stilbenes.[16] Among a variety of such photocyclizations simple azobenzenes and benzilidenanilines fail to undergo photocyclization under the usual conditions.[17] However, it has been reported that addition of sulfuric acid or Lewis acids dramatically promoted the formation of heterocyclic aromatic compounds.[18] There should be a distinct mechanistic difference between such acid-catalyzed photocyclization and the present ESIPT-induced photocyclizations, because in the photocyclization of **1a** and **1b** proton comes intramolecularly but it is not from external source.

Time-resolved IR spectroscopy

The occurrence of ESIPT is usually evidenced by observation of a strongly Stokes-shifted fluorescent emission.[19] Compound **1a** exhibits no fluorescence. However, we could probe the involvement of ESIPT by time-resolved IR spectroscopy,[12] which allowed the detection of the transient increase of the ground-state keto enamine form upon irradiation of **1a**. Fig. 5 shows the transient vibrational spectra of **1a** in carbon tetrachloride following excitation at 262 nm with a 5 ns pump pulse. The figure is represented in the form of a difference spectrum. Negative peaks represent a decrease of the infrared absorption due to the depletion of the ground state and positive peaks correspond to an increase of the absorption by the photogenerated transient species. Several new absorption bands appear following excitation. These absorptions arise from two species, one (1550 and 1540 cm^{-1}) decays rapidly and almost disappears at 200–300 μs delays, the other (1630 and 1245 cm^{-1}) decays very slowly and still remains at 800 μs delays. Hereafter we designate the former species as **A** and the latter as **B**, respectively.

After the time-resolved measurements photoproduct **2a** was not detected and **1a** was recovered. Thus all the spectral changes were reversible. Decay curves of each transient absorption and the recovery curve of **1a** are displayed in Fig. 6. The recovery of the ground-state **1a** corresponds with the decay of **B**, indicating that **1a** is reproduced at the expense of **B** as a precursor. Based on this analysis together with the IR absorption bands,[20] transient species **B** was assigned to the keto enamine tautomer in the ground state. Its 1630 cm^{-1} peak is attributed to the hydrogen-bonded C=O group, as observed at 1636 cm^{-1} in 1,5-dihydroxy-9,10-anthraquinone. Furthermore, **B** shows an absorption band at 1245 cm^{-1} which is attributable to the C–N stretching vibration. Curve fitting assuming a simple exponential decay afforded the time constant of 1.3 ms for the 1630 cm^{-1} absorption of **B**.

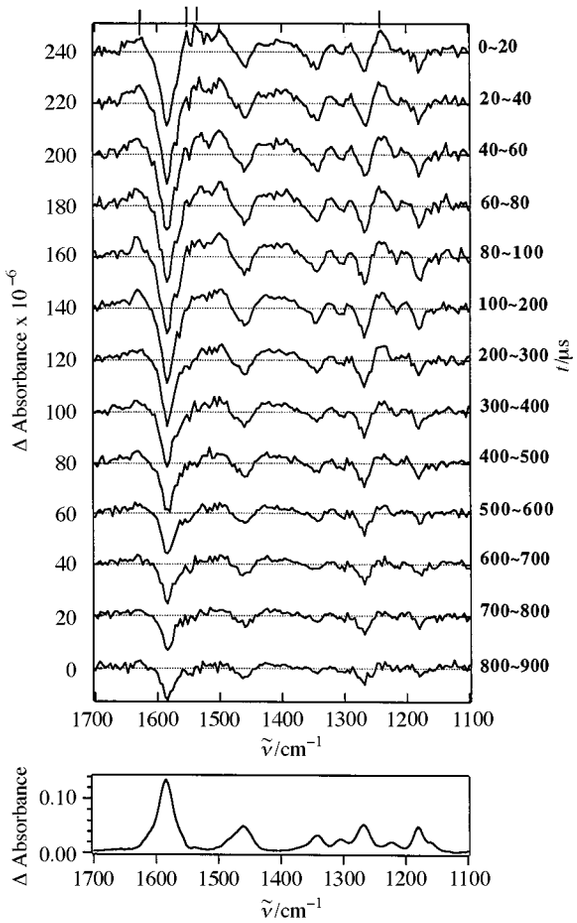

Fig. 5 Time-resolved IR spectra of **1a** after photoexcitation. Negative peaks represent a decrease in the absorption and positive peaks correspond to an increase in the absorption. The IR spectrum of **1a** is shown at the bottom.

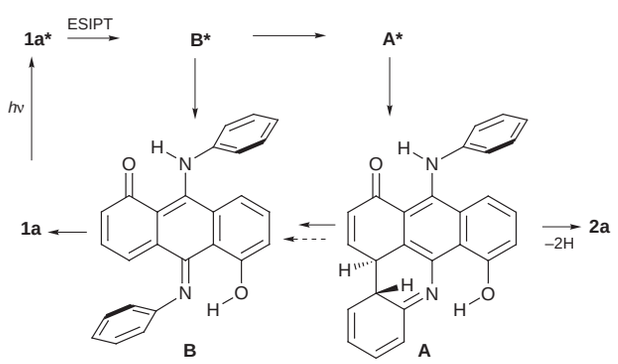

Scheme 1

With respect to transient species **A**, we presume a ring-closed product, a precursor to **2a** and back to **B** (Scheme 1), to be the most plausible candidate based on its infrared absorptions. Characteristic absorptions of **A** occur at 1550 and 1540 cm^{-1}. The absorption band at 1550 cm^{-1} corresponds well to that of the hydrogen-bonded C=N bond incorporated in a cyclic framework, as seen at 1551 cm^{-1} in **2a**. In contrast to the long lifetime of **B**, **A** has relatively short time constants of 92 and 82 μs for the 1550 and 1540 cm^{-1} bands, respectively.

Transient species **A** and **B** appear almost simultaneously with pumping and therefore all the steps to **A** and **B** occur in a rapid timescale and therefore it seems to be rational that the transient species **1a***, **B*** and **A*** could not be detected on a submicrosecond timescale. However, when we look closely the appearances of **A** and **B** (Fig. 7), there is clearly a delay in the generation of **B**, while **A** appears simultaneously with pumping.

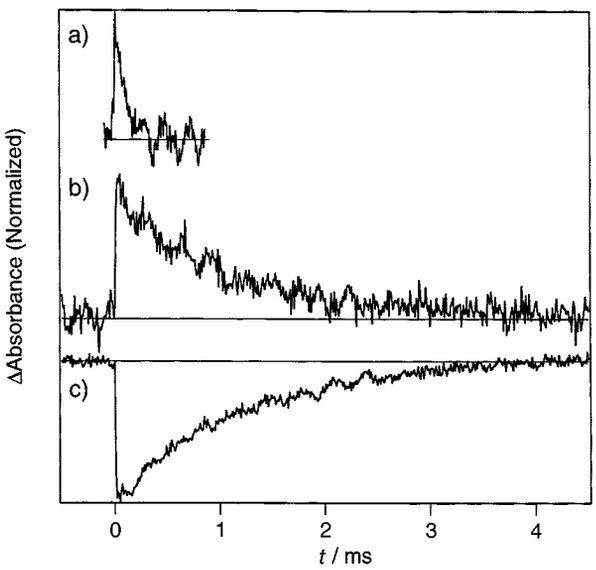

Fig. 6 Decay curves of the absorption bands at (a) 1550 cm^{-1} (transient species **A**) and (b) 1630 cm^{-1} (transient species **B**), and (c) recovery curve of the absorption band at 1585 cm^{-1} (**1a**)

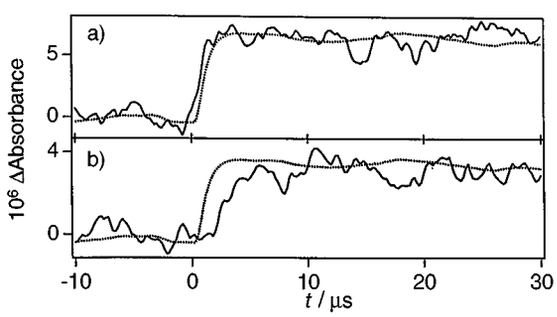

Fig. 7 Close look at initial portion of the decay curve of (a) **A** and (b) **B**

This observation indicates that **A** is not formed at the expense of **B**. Thus we postulate the progression of two excited states **B*** and **A*** as depicted in Scheme 1.

There is also a clear delay in the recovery curve of **1a** (Fig. 6): the increase of **1a** as monitored at 1585 cm^{-1} band starts with 100 μs delay after pumping. This profile indicates the involvement of another path that rapidly produces ground state **1a**: some **1a** has already been produced prior to recovery from **B**. It may be conceivable that photoexcited **1a** is rapidly deactivated to the ground state (from **1a*** to **1a**).

Oxidation is required to convert the transient species **A** to **2a**. This process was easily achieved by dissolved oxygen in the solvent. When argon bubbling was completely carried out to exclude oxygen, the photocyclization product was not obtained, as was the case in the time-resolved experiments. On the other hand, when argon was not bubbled, the formation of **2a** was confirmed by its UV absorption at 530 nm. In preparative-scale experiments, argon bubbling is regarded to be inefficient, since a large amount of solvent was used.

It should finally be noted that we observe the same photoexcited process in the time-resolved experiments induced by a 262 nm laser pulse and in the preparative experiments using a high pressure Hg lamp through a Pyrex filter. We carried out the time-resolved experiments at 349 nm by using a low concentration of **1a** in a CCl_4 solution under argon bubbling and could observe the decay of 1585 cm^{-1} absorption of **1a** with the time constant of 1 ms. This is consistent with the experiments using a 262 nm laser pulse. When argon was not bubbled, the formation of **2a** was ascertained by means of the UV absorption at 530 nm.

Conclusions

This study describes novel photochemical aromatic cyclizations of *N*,*N*′-diphenyl-1-hydroxy-9,10-anthraquinone diimines to give dibenzacridine derivatives. This type of photoreaction appears to proceed *via* similar processes to those observed in a variety of stilbene-type of compounds. However, chemical and photophysical evidence for the involvement of ESIPT has been demonstrated. In the latter, time-resolved IR spectroscopy detected the ground-state keto form as a transient species and its time constant for the reverse proton transfer was estimated to be 1.3 ms. There are few data for recovery lifetimes of the ground state keto form.[21] The value of 1.3 ms obtained in this work should be a reliable one, since the time-resolved IR spectroscopy observes directly this transient species. The present study indicates that a deactivation process other than tautomerisation is also involved for the ESIPT state.

References

1 For reviews, see special issues. *Chem. Phys.*, 1989, **136**; *J. Phys. Chem.*, 1991, **95**.
2 D. Le Gourrierec, S. M. Ormson and R. G. Brown, *Prog. React. Kinet.*, 1994, **19**, 211.
3 S. M. Ormson and R. G. Brown, *Prog. React. Kinet.*, 1994, **19**, 45.
4 M. C. Jimenez, P. Leal, M. A. Miranda and R. Tormos, *J. Org. Chem.*, 1995, **60**, 3243.
5 M. Isaks, K. Yates and P. Kalanderopoulos, *J. Am. Chem. Soc.*, 1984, **106**, 2728.
6 K. H. Grellmann and E. Tauer, *J. Am. Chem. Soc.*, 1973, **95**, 3104.
7 K. Kobayashi, M. Iguchi, T. Imakubo, K. Iwata and H. Hamaguchi, *Chem. Commun.*, 1998, 763.
8 For a recent example, see: S. M. Ormson, D. LeGourrierec, R. G. Brown and P. Foggi, *J. Chem. Soc.*, *Chem. Commun.*, 1995, 2133.
9 T. Yuzawa, H. Takahashi and H. Hamaguchi, *Chem. Phys. Lett.*, 1993, **202**, 221.
10 H. W. Boone, M. A. Bruck, R. B. Bates, A. B. Padias and H. K. Hall, Jr., *J. Org. Chem.*, 1995, **60**, 5279.
11 (*a*) teXsan: Crystal Structure Analysis Package, Molecular Structure Corporation, 1985; 1992; (*b*) M. C. Burla, M. Camalli, G. Cascarano, C. Giacovazzo, G. Polidori, R. Spagna and D. Viterbo, *J. Appl. Crystallogr*., 1989, **22**, 389.
12 K. Iwata, C. Kato and H. Hamaguchi, *Appl. Spectrosc.*, 1989, **43**, 16; K. Iwata and H. Hamaguchi, *Appl. Spectrosc.*, 1990, **44**, 1431.
13 A. Everaerts, S. Roberts and H. K. Hall, Jr., *J. Polym. Sci.*, *Polym. Chem. Ed.*, 1983, **24**, 1703.
14 For X-ray analyses of salicylideneanilines, see: T. Inabe, N. Hoshino, T. Mitani and Y. Maruyama, *Bull. Chem. Soc. Jpn.*, 1989, **62**, 2245; N. Hoshino, T. Inabe, T. Mitani and Y. Maruyama, *Bull. Chem. Soc. Jpn.*, 1988, **61**, 4207; T. Inabe, I. Gautier-Luneau, N. Hoshino, K. Okaniwa, H. Okamoto, T. Mitani, U. Nagashima and Y. Maruyama, *Bull. Chem. Soc. Jpn.*, 1991, **64**, 801.
15 For NMR spectra of salicylideneanilines, see: D. K. Zheglova, V. Gindin and A. I. Kol'tsov, *J. Chem. Res.* (*S*), 1995, 32; S. H. Alarcon, A. C. Olivieri and M. G. Sierra, *J. Chem. Soc.*, *Perkin Trans. 2*, 1994, 1067; S. H. Alarcon, A. C. Olivieri, G. R. Labadie, R. M. Cravero and M. Gonzalez-Sierra, *Tetrahedron*, 1995, **51**, 4619.
16 A. Gilbert, in *Synthetic Organic Photochemistry*, ed. W. M. Horspool, Plenum Press, New York, 1984, p. 1; B. Mallory and C. W. Mallory, in *Organic Reactions*, Wiley, New York, 1984, vol. 30.
17 G. Zimmerman, L. Chow and U. Paik, *J. Am. Chem. Soc.*, 1958, **80**, 3528.
18 F. B. Mallory and C. S. Wood, *Tetrahedron Lett.*, 1965, 2643; G. M. Badger, C. P. Joshua and G. E. Lewis, *Tetrahedron Lett.*, 1964, 3711; H. H. Perkampus and B. Behjati, *J. Heterocycl. Chem.*, 1974, **11**, 511; G. M. Thompson and S. Docter, *Tetrahedron Lett.*, 1988, **29**, 5213; C. P. Joshua and V. N. R. Pillai, *Tetrahedron*, 1974, **30**, 3333.
19 R. S. Becker and W. F. Richey, *J. Am. Chem. Soc.*, 1967, **89**, 1298; W. F. Richey and R. S. Becker, *J. Chem. Phys.*, 1968, **49**, 2092.
20 For IR spectra of salicylideneanilines, see: J. W. Ledbetter, Jr., *J. Phys. Chem.*, 1977, **81**, 54.
21 For a recent example, see: C. Chudoba, S. Lutgen, T. Jentzasch, E. Riedle, M. Woerner and T. Elsaesser, *Chem. Phys. Lett.*, 1995, **240**, 35.

Paper 8/02170H
Received 19*th March* 1998
Accepted 18*th May* 1998